A.I.83

83

METALLURGY, MECHANICAL

Krishan K. Chawla
Marc A. Meyers *New Mexico Institute of Mining and Technology*

GLOSSARY

Composite: Material consisting of two or more chemically distinct phases, of which one is the main load carrier and the other serves as a load-transfer medium.

Creep: Time-dependent deformation under load: important in metals at high temperatures.

Dislocation: Line imperfection in a crystalline solid by whose motion plastic deformation is accomplished.

Elastic strain: Strain that disappears upon removal of forces that caused it.

Fatigue: Phenomenon of deformation and fracture under cyclic loading (or straining).

Fracture: Separation or fragmentation of a body into two or more parts, under the action of stresses.

Grain boundary: Transition region between grains of a polycrystalline solid.

Microalloyed steels: Low-carbon steels (0.5–0.2% C, 0.6–1.6% Mn) containing about 0.1% of elements such as niobium, vanadium, or titanium.

Plastic strain: Strain that remains in a body after removal of forces that caused it.

Precipitation: Rejection of a second phase from a supersaturated solid solution.

Solid solution: Solid phase having foreign (solute) atoms distributed in a matrix (solvent) of metal atoms.

Toughness: Ability of a material to resist cracking.

Work hardening: Ability of a crystalline solid to become stronger with plastic deformation.

Mechanical metallurgy is an interface, rather than a technical or scientific discipline. It uses princples of mechanics and metallurgy with the objective of rationalizing, predicting, modifying, and describing the response of metals to external loads or internal stresses. There are four important aspects of this field.

1. Mechanics of deformation, in which deformation is treated in the sequence in which it takes place: elastic deformation, plastic deformation, and fracture.
2. Metallurgy of deformation, in which the structural imperfections responsible for the mechanical properties of metals are analyzed.
3. Strengthening mechanisms, which deals with work hardening, solid-solution hardening, precipitation and dispersion hardening, fiber reinforcement, martensite strengthening, grain-size strengthening, thermomechanical processing, order hardening, and texture strengthening.
4. Mechanical testing, which links mechanical properties and performance. Commonly performed mechanical tests include tensile and compressive testing, shear testing, fracture testing, hardness testing, fatigue testing, creep testing, and formability testing.

I. Mechanics of Deformation

When a metal is subjected to an increasing external load, it experiences an elastic (recoverable) deformation, plastic (nonrecoverable or permanent) deformation, and finally fracture occurs. The phenomena involved in these three different regimes are very different.

When the strain and stresses are elastic, the theory of elasticity can be used to obtain the relationships between them. An elastic strain is defined as a strain that disappears instantaneously once the forces that cause it are re-

moved. The elastic regime of deformation is characterized, in metals, by a proportionality between stress (σ) and strain (e), $\sigma = Ee$, where E is the Young's modulus; this simple relationship between stress and strain is called Hooke's law.

A. Elasticity

Stress is force per unit surface area. Nine *stress* components can be defined with reference to an elemental cube (Fig. 1). The component σ_{ij} is the force per unit area in the i direction on a face whose normal is j direction. The six components with $i \neq j$ are the shear stresses while the three components with $i = j$ are the normal stresses. The conditions of rotational equilibrium requires that $\sigma_{23} = \sigma_{32}$, $\sigma_{31} = \sigma_{13}$, and $\sigma_{12} = \sigma_{21}$. We can represent the *displacement* of a point by a vector

$$\mathbf{u} = [u_1, u_2, u_3]$$

where u_1, u_2, u_3 are the components of vector $\mathbf{u}$ and can be represented as projections of $\mathbf{u}$ on the x_1, x_2, x_3 axes. Strain is the ratio of change in length to initial length. The nine strain components can be written in terms of the first partial derivatives of displacement components:

Normal strains

$$e_{11} = \frac{\partial u_1}{\partial x_1}, \qquad e_{22} = \frac{\partial u_2}{\partial x_2}, \qquad e_{33} = \frac{\partial u_3}{\partial x_3}$$

Shear strains

$$e_{23} = e_{32} = \tfrac{1}{2}\left(\frac{\partial u_2}{\partial x_3} + \frac{\partial u_3}{\partial x_2}\right)$$

$$e_{31} = e_{13} = \tfrac{1}{2}\left(\frac{\partial u_3}{\partial x_1} + \frac{\partial u_1}{\partial x_3}\right)$$

$$e_{12} = e_{21} = \tfrac{1}{2}\left(\frac{\partial u_1}{\partial x_2} + \frac{\partial u_2}{\partial x_1}\right)$$

The magnitude of these components is much smaller than unity. Hooke's law describes the relationship between stress and strain in the linear elastic regime. This law states that each stress component is proportional to each strain. For isotropic solids, we can write the generalized Hooke's law as

$$\begin{aligned}
\sigma_{11} &= 2Ge_{11} + \lambda(e_{11} + e_{22} + e_{33}) \\
\sigma_{22} &= 2Ge_{22} + \lambda(e_{11} + e_{22} + e_{33}) \\
\sigma_{33} &= 3Ge_{33} + \lambda(e_{11} + e_{22} + e_{33}) \\
\sigma_{12} &= 2Ge_{12}, \qquad \sigma_{23} = 2Ge_{23}, \qquad \sigma_{13} = 2Ge_{13}
\end{aligned} \tag{1}$$

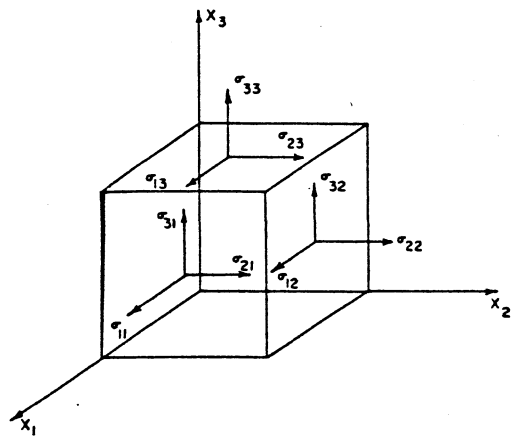

FIG. 1. Stresses acting on a unit cube.

where λ and G are the Lame constants; G is also the shear modulus. Notice that only two constants of proportionality are required for an isotropic solid. Engineers frequenty use other elastic constants, such as Young's modulus E, Poisson's ratio ν, and the bulk modulus K. For an isotropic material, only two constants are required. Thus, the constants E, G, ν, and K are interrelated. We have

$$E = 2G/(1 + \nu), \qquad K = E/3(1 - 2\nu),$$

$$\nu = \lambda/2(\lambda + G)$$

$$\nu = E\nu/(1 + \nu)(1 - 2\nu)$$

B. Plasticity

Once the stress corresponding to elastic limit of a metal is exceeded, permanent deformation is set in; that is, the deformation is not recovered on unloading. The plastic deformation is an irreversible process, and about 90% of the work of deformation is transformed into heat by internal dissipative processes, while the other 10% of the deformation energy is stored in the metal.

It is important to know the stress level at which a body starts to flow plastically, that is, the flow criterion for a general state of stress. In a uniaxial stress state, plastic flow starts when the stress-strain curve deviates from its initial linear elastic range. The material shape change resulting from plastic deformation (say, in rolling, forging, or wire drawing) does not depend significantly on hydrostatic stress, $\sigma_h = \frac{1}{3}(\sigma_1 + \sigma_2 + \sigma_3)$, but depends on the deviatoric stress component, $\sigma_{d_1} = (\sigma_1 - \sigma_h)$, etc. This is because plastic deformation of metals is accomplished by shear. [*See* PLASTICITY (ENGINEERING).]

A relation that satis
requirements of a pla

$$(\sigma_1 - \sigma_2)^2 + (\sigma_2 -$$

where σ_0 is the flow
uniaxial tension (or co
are principal stresses
originally proposed by
known as von Mises's
tic deformation is an
stresses and the strai
path-dependent—that i
affects the state of st
uses strain increments
total strain is obtaine
strain increments over
path. In lieu of Hooke'
ity the following three
ferred to the three prin

$$d\varepsilon_{p1} = dC[\sigma_1$$

$$d\varepsilon_{p2} = dC[\sigma_2$$

$$d\varepsilon_{p3} = dC[\sigma_3$$

where C represents a s
ter and the subscript p
nent. Poisson's ratio is
from the condition that
curs without any apprec
can be shown that

$$\sigma_1 - \tfrac{1}{2}(\sigma_2 + \sigma_3) =$$

and similarly for the oth
(2). This allows us to re

$$\frac{d\varepsilon_{p1}}{\sigma_{d1}} = \frac{d\varepsilon_{p2}}{\sigma_{d2}} =$$

Defining an effective str

$$\sigma_{eff} = \frac{\sqrt{2}}{2}[(\sigma_1 -$$

$$+ (\sigma_2 - \sigma_3$$

and an effective strain ir

$$d\varepsilon_{eff} = \frac{\sqrt{2}}{3}[(d\varepsilon_{p1} - d\varepsilon$$

$$+ (d\varepsilon_{p1} - d\varepsilon_{p2})$$

we can write

$$dC =$$

Equation (2) thus corres
with $\lambda = \frac{1}{2}$ and $1/E$ replac
Eq. (3). This parameter C

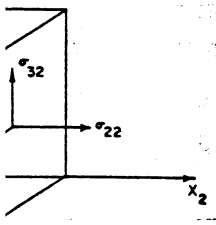

ɔn a unit cube.

constants; G is also
that only two con-
required for an iso-
enty use other elas-
ung's modulus E,
ılk modulus K. For
/o constants are re-
E, G, ν, and K are

$= E/3(1 - 2\nu)$.

ding to elastic limit
ıanent deformation
ation is not recov-
c deformation is an
ut 90% of the work
l into heat by inter-
ile the other 10% of
ɔred in the metal.
the stress level at
plastically, that is,
ıl state of stress. In
c flow starts when
tes from its initial
erial shape change
ıation (say, in roll-
;) does not depend
tress, $\sigma_h = \frac{1}{3}(\sigma_1 +$
e deviatoric stress
:tc. This is because
is accomplished by
GINEERING).]

A relation that satisfies fairly well the various requirements of a plastic flow criterion is

$$(\sigma_1 - \sigma_2)^2 + (\sigma_2 - \sigma_3)^2 + (\sigma_3 - \sigma_1)^2 = 2\sigma_0^2$$

where σ_0 is the flow stress of the material in uniaxial tension (or compression) and σ_1, σ_2, σ_3 are principal stresses. This relationship was originally proposed by Huber and is commonly known as von Mises's criterion. Since the plastic deformation is an irreversible process, the stresses and the strains in the final state are path-dependent—that is, the deformation history affects the state of strain. Consequently, one uses strain increments $d\varepsilon_{ij}$ in plasticity, and the total strain is obtained by summing up these strain increments over the whole deformation path. In lieu of Hooke's law, we have in plasticity the following three differential equations referred to the three principal axes:

$$\begin{aligned} d\varepsilon_{p1} &= dC[\sigma_1 - \tfrac{1}{2}(\sigma_2 + \sigma_3)] \\ d\varepsilon_{p2} &= dC[\sigma_2 - \tfrac{1}{2}(\sigma_3 + \sigma_1)] \\ d\varepsilon_{p3} &= dC[\sigma_3 - \tfrac{1}{2}(\sigma_1 + \sigma_2)] \end{aligned} \qquad (2)$$

where C represents a strain-dependent parameter and the subscript p denotes a plastic component. Poisson's ratio is taken as $\frac{1}{2}$, which follows from the condition that plastic deformation occurs without any appreciable volume change. It can be shown that

$$\sigma_1 - \tfrac{1}{2}(\sigma_2 + \sigma_3) = \tfrac{3}{2}(\sigma_1 - \sigma_h) = \tfrac{3}{2}\sigma_{d1}$$

and similarly for the other two relations in Eq. (2). This allows us to rewrite Eq. (2) as

$$\frac{d\varepsilon_{p1}}{\sigma_{d1}} = \frac{d\varepsilon_{p2}}{\sigma_{d2}} = \frac{d\varepsilon_{p3}}{\sigma_{d3}} = \tfrac{3}{2}\,dC$$

Defining an effective stress

$$\sigma_{eff} = \frac{\sqrt{2}}{2}[(\sigma_1 - \sigma_2)^2 + (\sigma_1 - \sigma_3)^2 + (\sigma_2 - \sigma_3)^2]^{1/2}$$

and an effective strain increment

$$d\varepsilon_{eff} = \frac{\sqrt{2}}{3}[(d\varepsilon_{p1} - d\varepsilon_{p2})^2 + (d\varepsilon_{p1} - d\varepsilon_{p2})^2 + (d\varepsilon_{p2} - d\varepsilon_{p3})^2]^{1/2}$$

we can write

$$dC = \frac{\sigma_{eff}}{d\varepsilon_{eff}} \qquad (3)$$

Equation (2) thus corresponds to Hooke's law with $\lambda = \frac{1}{2}$ and $1/E$ replaced by dC as defined in Eq. (3). This parameter C can be obtained as the inverse of the slope of an effective stress–effective strain curve.

Various technologically important deformation processes, such as rolling, forging, extrusion, and drawing, involve substantial plastic deformation, and the material response will depend on their plastic behavior. Application of plasticity theory helps in analyzing the stresses and strains involved. The use of computers in analysis of deformation processing has increased dramatically; examples of approaches made possible by the use of numerical methods are slip-line field theory, the upper bound method, and the finite element method. The reader is referred to the bibliography for details in this regard.

C. Fracture and Fracture Toughness

Fracture is the culmination of the deformation process of a metal. We can define the separation or fragmentation of a metal into two or more parts, under the action of stresses, as fracture. The principal ways in which a metal may fracture are:

1. slow application of external loads,
2. rapid application of external loads (impact),
3. cyclic loading (fatigue), and
4. environmentally assisted cracking (hydrogen embrittlement, stress corrosion, etc.).

In any given situation, the process of fracture may be conveniently subdivided into the three stages:

(a) damage accumulation,
(b) nucleation of one or more cracks, and
(c) propagation of a crack to complete separation of the material.

The damage accumulation is associated with the material properties, such as its atomic structure, crystal lattice, and grain boundaries, and the loading history. When the local strength or ductility is exceeded, a crack (two free internal surfaces) is formed. On continued loading, the crack propagates through the section until complete rupture. This last stage of fracture, crack propagation, has been very fruitfully explored by using concepts of fracture mechanics [*See* FRACTURE AND FATIGUE.]

Inglis, in 1913, calculated the stress distribution in an elastic plate containing an elliptical crack of length $2a$ subjected to a tensile stress σ (Fig. 2). The Inglis formula says that the maxi-

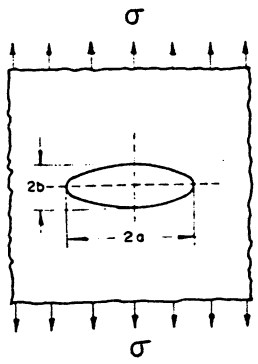

FIG. 2. Griffith model of a crack.

mum stress occurs at the ends of the major axis of the elliptical cavity,

$$\sigma_{max} = \sigma\left(1 + \frac{2a}{b}\right)$$

where $2a$ and $2b$ are the major and the minor axes of the ellipse, respectively. In the case of an extremely flat ellipse (i.e., a very narrow crack) of length $2a$ and having a radius of curvature, $\rho = b^2/a$, we can rewrite the above equation as

$$\sigma_{max} = \sigma\left(1 + 2\frac{\sqrt{a}}{\rho}\right) \approx 2\sigma\frac{\sqrt{a}}{\rho} \quad \text{for} \quad \rho \ll a \tag{4}$$

Griffith calculated the decrease in energy due to the presence of a crack in the plate according to the Inglis formulation and found it to be equal to $U(\sigma) = \pi\sigma^2a^2/E$ per unit thickness of the plate. Griffith realized that the crack would propagate by extending its length when the stress attained a critical value, σ_c. The presence of two new (crack) surfaces would result in an increase in energy equal to $U(\gamma) = 4\gamma a$, where γ is the specific surface energy of the crack forces. The crack would grow when $\partial U(\sigma)/\partial a$ just exceeded $\partial U(\gamma)/\partial a$, that is, when the decrease of elastic deformation energy was greater than the increase of surface energy due to crack extension. This leads to

$$\sigma_c = \sqrt{2\gamma E/\pi a} \tag{5}$$

We note that the tensile fracture stress σ_c is proportional to $a^{-1/2}$ and that the quantity $\sigma_c\sqrt{a}$ depends only on the material constants. Thus, from Eqs. (4) and (5), we have

$$\sigma_c\sqrt{a} = \tfrac{1}{2}(\sigma_{max})_c\sqrt{\rho} = \text{constant}$$

where the subscript c denotes the fracture condition. The quantity $\sigma_c\sqrt{a}$ is a measure of fracture toughness (K_c) of the material.

The fundamental work of Inglis and Griffith has been extended into the disciplines of linear-elastic fracture mechanics (LEFM) and elasto-plastic fracture mechanics (EPFM). The discipline of fracture mechanics has had a steady increase in technological importance, as we move from the "weaker" (and more ductile) materials to materials with greater and greater strength (and, alas, less ductility). Failure in "weaker" materials occurs primarily by void nucleation, growth, and coalescence, and is called "ductile." The relevant design criterion for such materials is the yield stress. High-technology materials, on the other hand (metal-matrix composites, high-strength steels, etc.) fail by crack propagation, and the existence of flaws (or cracks) can dramatically affect the failure stress, to levels significantly below the yield stress. Thus, the fracture toughness becomes the most important design parameters and a maximum allowable flaw size is specified. In fracture mechanics, we model a crack as a slit in a continuum. The stresses at a point in the crack tip vicinity are given in terms of a parameter called the stress intensity factor K_I,

$$\sigma_{ij} = (K_I/\sqrt{2\pi r})\, f_{ij}(\theta) \tag{6}$$

where r is the distance of the point from the crack tip, θ is the angle of the point from the crack plane, and $f_{ij}(\theta)$ is a function of the angle θ. The term K_I is a function of the crack geometry and the applied stress. In brittle, that is, linear-elastic, materials with very limited crack tip plasticity, fracture occurs when K_I reaches a critical value K_{Ic}, the plane strain fracture toughness of the material. The term K_{Ic} is a material constant, and typical values of some metals and alloys are given in Table I. Also given in Table I is the respective yield stress σ_y value as a point of reference. LEFM also treats the problem of crack propagation from an energy viewpoint. According to this, fracture occurs when the crack extension force (or strain energy release rate) attains a critical value G_c. The term G is defined as $\partial U/\partial A$ where U is the total mechanical energy of the system and A is the area of the crack surface. In brittle materials, $G_c = 2\gamma$. The stress intensity and the energy approaches to fracture are equivalent, and $K_I^2 = EG_I$ under plane stress conditions. [*See* EMBRITTLEMENT, ENGINEERING ALLOYS.]

For the nonlinear elastic material, one can express the strain energy release rate as the line integral J, due to Rice. The integral J is evaluated around a path Γ surrounding the crack tip.

in counterclockwise
point on the lower cr

$$J = \int_\Gamma \{W\, d$$

where W is the strain
($W = \int^{\varepsilon_{mn}} \sigma_{ij}\, d\varepsilon_{ij} =$
stress-strain curve), T
U is the displacement
tour Γ. The important
material is that the J
dent; J characterizes
and is a measure of t
rate. As it should J redu
material.

Wells made a great a
tic fracture mechanics
fracture occurs when t
of opposite crack face
displacement (COD), a
The minimum radius o
crack is given by

$$r_y = \frac{1}{2\pi}$$

Suppose now, for simp
zone, in plane stress, is
have a "notional" crack
crack tip at a distance r
Then, we have the strain
given by $\varepsilon_y = \sigma_y/E$ (ci
elastic/plastic boundary).
by

$$\delta = \varepsilon_y(\text{gag}$$
$$= \varepsilon_y(2\pi r$$
$$= \varepsilon_y\left(\frac{K^2}{\sigma_y^2}\right.$$

ork of Inglis and Griffith
o the disciplines of linear-
inics (LEFM) and elasto-
inics (EPFM). The disci-
hanics has had a steady
gical importance, as we
r" (and more ductile) ma-
vith greater and greater
ess ductility). Failure in
occurs primarily by void
nd coalescence, and is
relevant design criterion
e yield stress. High-tech-
ne other hand (metal-ma-
strength steels, etc.) fail
nd the existence of flaws
itically affect the failure
ficantly below the yield
ture toughness becomes
esign parameters and a
aw size is specified. In
model a crack as a slit in
ses at a point in the crack
in terms of a parameter
ity factor K_I,

$\sqrt{2\pi r})\, f_{ij}(\theta)$ (6)

e of the point from the
le of the point from the
s a function of the angle
tion of the crack geome-
ss. In brittle, that is, lin-
th very limited crack tip
urs when K_I reaches a
plane strain fracture
l. The term K_{Ic} is a ma-
ypical values of some
given in Table I. Also
spective yield stress σ_y
ence. LEFM also treats
ropagation from an en-
ing to this, fracture oc-
tension force (or strain
ins a critical value G_c.
$\partial U/\partial A$ where U is the
of the system and A is
rface. In brittle mate-
ss intensity and the en-
icture are equivalent,
lane stress conditions.
. ENGINEERING AL-

ic material, one can ex-
elease rate as the line
he integral J is evalu-
ounding the crack tip,

TABLE I. K_{Ic} and σ_y of Some Metals and Alloys at Ambient Temperature

Material	σ_y (MPa)	K_{Ic} (MPa $\sqrt{m}$)
Al–4% Cu	405	26
Al–3% Mg–7% Zn	500	25
Ti–6% Al–1% V	850	60
Ti–6% Al–4% V	1020	52
Stainless steel (18–8)	340	200
A533 steel (0.25% C, 1.3% Mn)	450	120
12% Cr steel	1550	50
Maraging steel (18% Ni, 8% Co, 4% Mo)	1930	74
Cast iron	250	20

in counterclockwise direction, starting from a point on the lower crack surface,

$$J = \int_\Gamma \{W\, dy - T(\partial U/\partial x)\, ds\} \qquad (7)$$

where W is the strain energy density function ($W = \int^{\varepsilon_{max}} \sigma_{ij}\, d\varepsilon_{ij}$ = area under the non-linear stress-strain curve), T is the traction vector, and U is the displacement on a length ds of the contour Γ. The important point for nonlinear elastic material is that the J integral is path-independent; J characterizes the crack tip stress field and is a measure of the elastic energy release rate. As it should J reduces to G for linear elastic material.

Wells made a great advance in the elasto-plastic fracture mechanics when he proposed that fracture occurs when the relative displacement of opposite crack faces, called crack opening displacement (COD), attains a critical value δ_c. The minimum radius of the plastic zone at the crack is given by

$$r_y = \frac{1}{2\pi}\left(\frac{K}{\sigma_y}\right)^2 \qquad (8)$$

Suppose now, for simplicity, that the plastic zone, in plane stress, is cylindrical and that we have a "notional" crack of length $(a + r_y)$ with crack tip at a distance r_y ahead of the real tip. Then, we have the strain around the plastic zone given by $\varepsilon_y = \sigma_y/E$ (circumference being the elastic/plastic boundary). The COD is then given by

$$\begin{aligned}\delta &= \varepsilon_y(\text{gage length}) \\ &= \varepsilon_y(2\pi r_y) \\ &= \varepsilon_y\left(\frac{K^2}{\sigma_y^2}\right)\end{aligned}$$

or

$$\delta = K^2/\sigma_y E \qquad (9a)$$

or

$$G = \sigma_y \delta \qquad (9b)$$

Similar results are obtained for COD using the so-called Dugdale–Bilby–Cottrell–Swinden model of the crack.

Although the concept of COD does represent a great advance into the plastic regime, it does not have the strain-energy release character of K and G (or J) in the elastic regime. The parameters G, J, δ, and K are identical in characterizing the crack tip region "for any one configuration in a constant stress state and constant ratio of in-plane stresses."

II. Metallurgy of Deformation

The theoretical strength calculations of perfect crystals indicated that the ideal strength value should be of the order of gigapascals (GPa), whereas the real strength of metals is orders of magnitude below this level. The great breakthrough event in understanding this difference was the idea of dislocations introduced in 1934. In fact, not only dislocations but also the various defects existing in metals and their interactions are responsible for this discrepancy between the real and theoretical strength values. We can classify the structural defects as per their dimensionality as (Fig. 3):

1. point defects (zero-dimensional),
2. line defects (unidimensional),
3. planar or interfacial defects (bidimensional), or
4. volume defects (tridimensional).

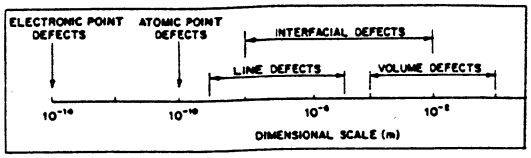

FIG. 3. Dimensional ranges of different classes of defects.

Point defects can be of three types. A *vacancy* is created when an atomic position in the crystal lattice is vacant. An *interstitial* is produced when an atom of the material or a foreign atom occupies an interstitial or nonlattice position. A *substitutional* point defect comes into being when a regular atomic position is occupied by a foreign atom. [*See* CRYSTALLOGRAPHY.]

Intrinsic point defects (vacancies and self-interstitials) in metals exist at a given temperature in equilibrium concentrations. Increased concentrations of these defects can be produced by quenching from high temperatures, bombarding with energetic particles such as neutrons, and plastic deformation. Point defects can have a marked effect on the mechanical properties.

The line imperfections called dislocations have been one of the important conceptual developments in the area of mechanical metallurgy. A dislocation is defined by two vectors: a dislocation line vector (tangent to the line), and its Burgers vector, which gives the direction of atomic displacement. The dislocation has a kind of lever effect, as it allows by its movement one part of metal to be sheared over the other without the need for simultaneous movement of atoms across a plane. It is the presence of these line imperfections that makes it so easy to deform the metals plastically. Under normal circumstances then, the plastic deformation of metals is accomplished by the movement of these dislocations. Figure 4(a) shows an edge dislocation. The two vectors, defining the dislocation line and the Burgers direction, are designated as **t** and **b**, respectively. The vector **t** [not shown in Fig. 4(a)] is perpendicular to **b**. The dislocation can produce shear in metals at stresses much below the stresses required for simultaneous shear across a plane, and Fig. 4(b) shows this in an analogy. A carpet can be moved by pushing. However, a much lower force is required to move the carpet by a distance b if a defect is introduced into it and made to move the whole extension at the carpet. Figure 5 shows

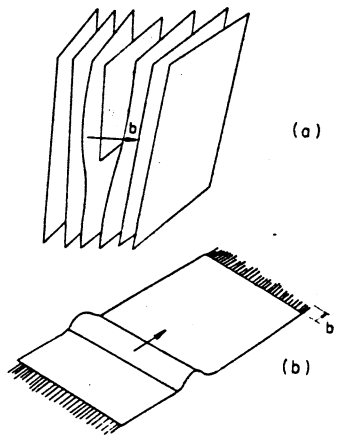

FIG. 4. (a) Schematic illustration of an edge dislocation with Burgers vector **b**. (b) Analogy of an imperfection moving along a carpet and producing displacement **b**.

dislocations as seen by transmission electron microscopy in a thin foil of aluminum. The dislocations can be seen as dark lines. They are visible in the transmission electron microscope because of the distortion of the atomic planes. This aluminum specimen is in the deformed condition and therefore exhibits quite a high density of dislocations.

The interfacial or planar defects occupy an area or surface of the crystal, for example, grain boundaries, twin boundaries, and domain and antiphase boundaries. Grain boundaries are, by far, the most important of these planar defects from the mechanical metallurgy point of view.

Among the volumetric or tridimensional de-

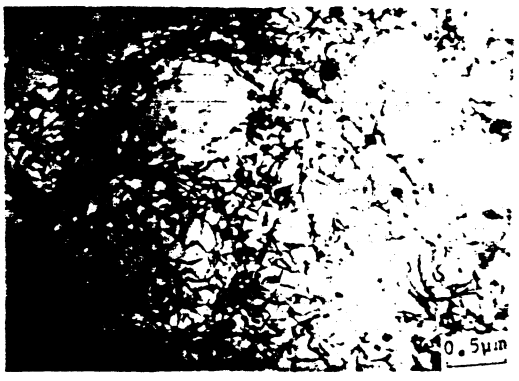

FIG. 5. Dislocations (dark lines) in aluminum (transmission electron micrograph).

fects we can inclu
bles, etc.

All these imperfe
on the mechanical
be discussed in Sec

III. Strengtheni

Experimental res
ing (or strain harden
metal to get more re
deformed, is relate
dislocation density (
exists a linear relati
(τ) and $\sqrt{\rho}$:

$$\tau = \tau$$

where τ_0 is the shea
dislocation in the ab
Basically, work hard
teractions among dis
ent slip planes. A ta
results after a small p
pedes the motion of
turn, requires higher
formation. There exis
posed to explain the
with various kinds
grain boundaries, sc
etc.) that result in cha
of metals. All of these
tion between τ and ρ g
thereby that a particul

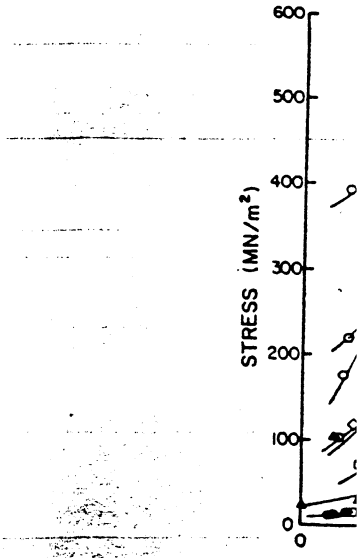

fects we can include large inclusions, gas bubbles, etc.

All these imperfections have a strong bearing on the mechanical properties of metals, as will be discussed in Section III.

III. Strengthening Mechanisms

Experimental results show that work hardening (or strain hardening), which is the ability of a metal to get more resistant to deformation as it is deformed, is related in a singular way to the dislocation density (ρ) after deformation. There exists a linear relation between the flow stress (τ) and $\sqrt{\rho}$:

$$\tau = \tau_0 + \alpha G b \sqrt{\rho} \qquad (10)$$

where τ_0 is the shear stress required to move a dislocation in the absence of other dislocations. Basically, work hardening results due to the interactions among dislocations moving on different slip planes. A tangled dislocation network results after a small plastic deformation that impedes the motion of other dislocations. This, in turn, requires higher loads for further plastic deformation. There exist a number of theories proposed to explain the interaction of dislocations with various kinds of barriers (dislocations, grain boundaries, solute atoms, precipitates, etc.) that result in characteristic strain hardening of metals. All of these theories arrive at the relation between τ and ρ given in Eq. (10), indicating thereby that a particular dislocation distribution is not crucial, and that strain hardening in practice is a statistical result of some factor that remains the same for various distributions. Cold working of metals leading to strengthening due to work hardening is a routinely used strengthening technique.

A similar relationship exists between the flow stress τ and the mean grain size (or dislocation cell size):

$$\tau = \tau_0 + \alpha' G b D^{-1/2} \qquad (11)$$

where D is the mean grain diameter. This relationship is known as the Hall–Petch relationship, after the two researchers who first discovered it. Hall–Petch plots for a number of metals and alloys are shown in Fig. 6.

Again, various models have been proposed to explain this square-root dependence on grain size. Earlier explanations involved a dislocation pile-up bursting through a grain boundary due to stress concentrations at the pile-up tip and activation of dislocation courses in adjacent grains. Later theories involved the activation of grain-boundary dislocation sources and pumping of dislocations into grain interiors, elastic incompatibility stresses between adjacent grains leading to localized plastic flow at the grain boundaries, etc. An important aspect strengthening by grain refinement is that, unlike other strengthening mechanisms, it results in an improvement in toughness concurrent with that in strength.

Other internal impediments to dislocation motion having effects analogous to that of grain

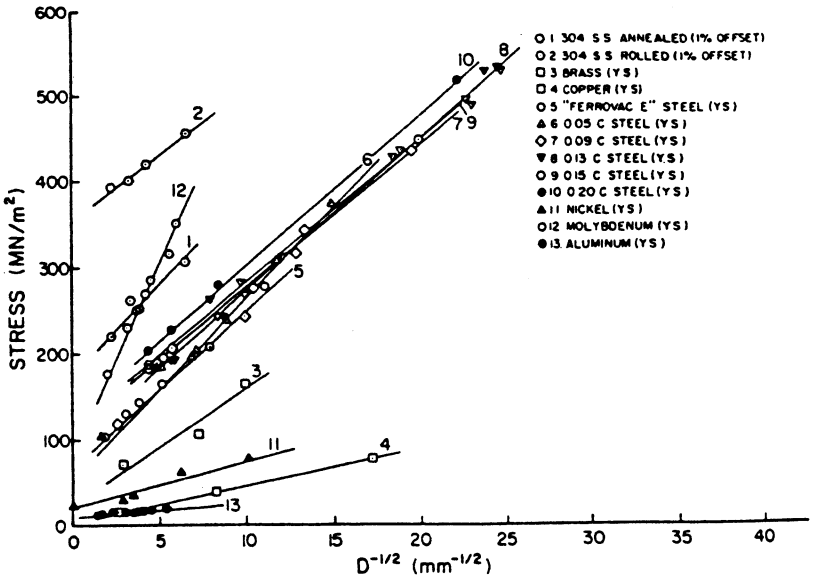

FIG. 6. Hall–Petch plot for a number of metals and alloys.

boundaries are dislocation cell walls and twin boundaries. Dislocation cell structure consists of tangles of dislocations arranged in walls surrounding regions almost free of dislocations. A twin boundary is a special kind of low-energy boundary. Their effect on flow stress may be represented by

$$\sigma = \sigma_0 + K\Delta^{-m}$$

where Δ represents the substructure dimensions (say, the cell size) and the coefficient m has been found to vary between $\frac{1}{2}$ and 1.

Another easy way of strengthening metals by impeding dislocation motion is that of introducing heterogeneities such as solute atoms or precipitates or hard particles in a ductile matrix. When one introduces solute atoms (say, C, N, or Mn, in Fe), we obtain solid-solution hardening. Interstitial solutes such as C and N are much more efficient strengthening agents than substitutional solutes such as Mn and Si. This is so because the former cause a tetragonal distortion in the lattice and thus interact with both screw and edge dislocation, while the latter cause a spherical distortion, which only interacts with edge dislocations, as the screw dislocations have a pure shear stress field and no hydrostatic component.

Precipitation hardening of a metal is obtained by making a supersaturated solid solution reject a finely distributed second phase. Classical examples of precipitation strengthening are those of Al–Cu, Al–Zn–Mg alloys, which are extensively used in the aircraft industry. Oxide dispersion strengthening involves artificially dispersing rather small volume fractions of strong and inert oxide particles (Al_2O_3, SiO_2, ThO_2, etc.) in a ductile matrix by internal oxidation or powder metallurgy techniques. Both the second-phase precipitates and dispersoids act as barriers to dislocation motion in the ductile matrix, thus making the matrix stronger. Dispersion-hardened systems (e.g., Al + Al_2O_3) show high strength levels at elevated temperatures, while precipitates (say, $CuAl_2$ in Al) tend to dissolve at those temperatures. Precipitation hardening systems, however, have the advantage of enabling one to process the alloy in a soft stage and give the precipitation treatment to the finished part. [*See* PHASE TRANSFORMATIONS. CRYSTALLOGRAPHIC ASPECTS.]

An important success story in the area of mechanical metallurgy of the 1960s and 1970s is that of strong and tough microalloyed steels (low carbon–manganese steels containing Nb, V, or Ti). The way to obtain strong yet tough steels without increasing the C content (which makes welding difficult) and large contents of alloying elements (expensive) is to subject these steels to what has been called "controlled rolling." Controlled rolling is nothing but a sequence of giving controlled amounts of deformations by hot-rolling at specific temperatures followed by controlled cooling. The objective is to obtain a fine ferritic grain size (a few micrometers). The ferritic grain size obtained after austenization and cooling depends on the initial austenitic grain size, as the ferrite nucleates preferentially at the austenite boundaries. Ferrite (BCC) is the low-temperature phase, while austenite (FCC) is the high-temperature phase in the Fe–C system. The ferrite grain size also depends on the austenite(γ) → ferrite(α) transformation temperature. Lower transformation temperatures favor the nucleation rate, resulting in a large number of ferritic grains (i.e., very small ferritic grain size). The controlled-rolling processing exploits the capacity of very small amounts (microalloying elements) of Nb, V, Ti, etc., to precipitate as extremely fine precipitates in austenite and thus retard the recrystallization and/or impede the grain growth of austenite. This leads to a posterior ferrite grain refinement, which results in strengthening as per the Hall–Petch relationship, as well as in improved toughness.

Precipitation or dispersion hardening of a metal can result in a dramatic increase in the yield stress and/or the work hardening rate. The influence of these obstacles on the elastic modulus is negligible. This is so because the intrinsic properties of the strong particles (e.g., the high elastic modulus) are not utilized.

The general idea of fiber reinforcement of metals is to use the higher load-bearing capacity of the strong fibrous phase. The 1960s and 1970s saw the advent of many advanced fibers such as boron, carbon, silicon carbide, alumina, etc., which are very light and have an extremely high elastic modulus. The matrix in a fibrous composite has the important function of transmitting the applied force to the principal load-bearing component, the fiber, in addition to serving as a binder. Some of the important metal matrix composite systems and their applications are presented in Table II.

Quenching of steel to produce a martensitic phase has been a time honored strengthening mechanism for steels. The underlying detailed mechanisms explaining this phenomenon have become understood only recently. These insights have led to some novel uses of martensitic transformation. In the transformation-induced plasticity (TRIP), the martensitic transformation occurs during deformation and serves to

TABLE II. S

Fi (subs
Boron (W)
Borsic
Boron (C)
Boron carbid boron
Rayon T50
PAN HTS T3
PAN HM
Pitch P
Pitch LIHM
FP alumina
Silicon carbide
Silicon carbide
Silicon carbide
Tungsten
WReHfC
W1.5ThO_2
Molybdenum
Ni_3Al–Ni_3Nb
TaC, Cr_3C_2
Nb_3Sn, V_3Ga, N

strengthen the regior
neck, and thus the d
any deterioration of
has been successfull
tially stabilized zirc
ness dramatically.
shape-memory effec
upon being plastically
ternal changes in the
tensite plates such th
initial shape.

Thermomechanical
an all encompassing
involving introductio
the thermal treatmen
that alters the proces
mal treatment and im
way of illustration, w
treatments. Maraging
attain a yield strengt
steel whose typical c
Mo, 0.5% Ti, 8% Co,
tensite produced by c
tively ductile, as it doe
can be easily process
precipitation hardened
metallic compounds c

TABLE II. Some Metal Matrix Composite Systems and Their Applications

Fiber (substrate)	Matrix	Applications
Boron (W) Borsic Boron (C) Boron carbide-coated boron	Al, Mg, Ti Al, Ti Al, Mg, Ti Al, Mg, Ti	Compressor blades, jet engine fan blades, antennae structures, high-temperature structures
Rayon T50 PAN HTS T300 PAN HM Pitch P Pitch LIHM	Al, Mg, Pb, Cu	Satellite, missile, and helicopter parts; space and satellite structures; storage battery plates; electrical contacts
FP alumina	Al, Mg, Pb	Storage battery plates, helicopter components
Silicon carbide (W) Silicon carbide (C) Silicon carbide	Al, Ti Al, Ti Al, Ti	High-temperature structures, high-temperature engines, components
Tungsten WReHfC W1.5ThO_2 Molybdenum Ni_3Al–Ni_3Nb TaC, Cr_7C_3	 Superalloy Superalloy Superalloy Superalloy	 High-temperature turbine components
Nb_3Sn, V_3Ga, NbTi	Cu	Superconductors

strengthen the regions ahead of a crack or near a neck, and thus the ductility is enhanced without any deterioration of strength. The TRIP concept has been successfully applied to a ceramic, partially stabilized zirconia, increasing its toughness dramatically. Another example is the shape-memory effect, wherein the material, upon being plastically deformed, undergoes internal changes in the configuration of the martensite plates such that heating recomposes the initial shape.

Thermomechanical processing or treatment is an all encompassing title for various processes involving introduction of plastic deformation in the thermal treatment cycle of a metal in a way that alters the processes occurring during thermal treatment and improves the properties. By way of illustration, we cite here a few of such treatments. Maraging treatment allows one to attain a yield strength of up to 2100 MPa in a steel whose typical composition is 18% Ni, 5% Mo, 0.5% Ti, 8% Co, and the rest Fe. The martensite produced by cooling such a steel is relatively ductile, as it does not contain carbon. This can be easily processed mechanically and then precipitation hardened by precipitation of intermetallic compounds of Ni, Mo, and Ti. TRIP steels already mentioned can also be classified in this category. Yet another example is a class of steels called dual-phase steels. These steels (compositions close to those of microalloyed steels) are quenched from a suitable temperature in the (ferrite and austenite) region of the Fe–C phase diagram such that the typical ferrite–pearlite microstructure of such steels is replaced by an essentially ferrite–martensite structure. Dual-phase steels display an excellent combination of strength and ductility and are very attractive to the automobile industry in its weight-reducing efforts.

If the atomic species, say A and B, of an alloy are arranged in a random manner, the alloy is said to be disordered. There is a fairly large number of alloys in which it is energetically favorable for atoms A and B to segregate to preferred lattice sites below a critical temperature and in well-defined atomic proportions (AB_3, AB, etc.) Mechanical properties of alloys are altered when they have an ordered structure, as illustrated by the Hall–Petch relationship for Ni_3Mn (Fig. 7). Gamma-prime strengthened superalloys form an important class of alloys showing the effect of ordering on strength.

Most metals are polycrystals. When a poly-

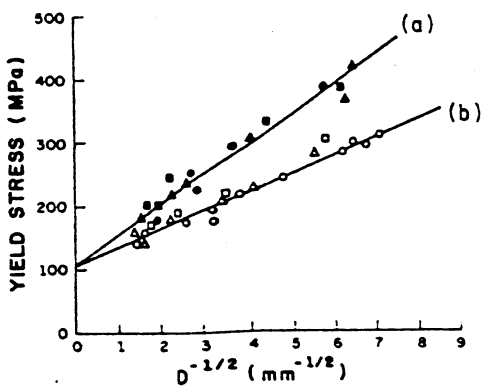

FIG. 7. Hall–Petch relationship for ordered (curve a) and disordered (curve b) alloys of Ni_3Mn. [After T. L. Johnson, R. G. Davies, and N. S. Stoloff (1965). *Phil. Mag.* **12**, 305.]

crystal is mechanically worked (rolling, forging, drawing, etc.), the randomly oriented grains (single crystals) slip on their appropriate slip systems and, thus, rotate from their initial orientation under constraint from neighboring grains. Thus, a strong preferred orientation or texture develops after large strains. A strongly textured material can exhibit highly anisotropic properties; a controlled anisotropy in sheet metals is exploited to obtain an improved final product. Although Young's modulus can only be affected slightly by texture, many other mechanical properties do show a marked orientation dependence. The rather marked orientation dependence of yield strength and strain to fracture of rolled copper sheet is shown in Fig. 8. Use is made of texture development in Fe–3% Si lami-

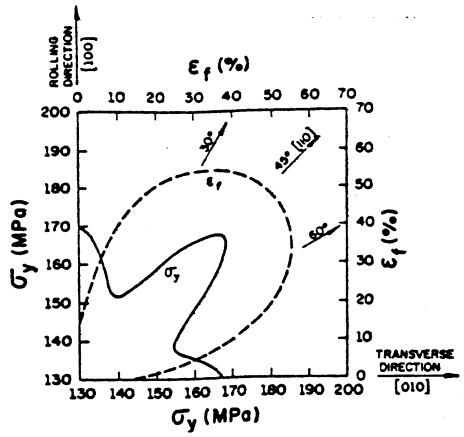

FIG. 8. Orientation dependence of yield strength σ_y and strain to fracture ε_f of a rolled copper sheet.

nations for transformer cores wherein thermomechanical treatments are given to develop a desirable magnetic anisotropy that improves the electrical performance.

A novel approach to obtaining enhanced mechanical performance is rapid solidification processing. By cooling metal at rates in the 10^4–10^6 K sec^{-1} range, it is possible to produce microstructures that are unique. Very fine powders or ribbons of rapidly solidified materials are processed into bulk material by hot pressing, hot isostatic pressing, or hot extrusion. The rapidly solidified materials can be amorphous (noncrystalline), microcrystalline (grain size below 1 μm), microdendritic solid solutions, containing solute concentrations vastly superior to those of conventionally processed materials can be obtained. Effectively, massive second-phase particles are totally eliminated. These unique microstructures lead to very favorable mechanical properties.

So far, we have only discussed monotonic strength and strengthening mechanisms operating at ambient temperatures. Quite frequently, however, the service conditions involve high temperatures (creep) and cyclic loading conditions (fatigue). A brief review of these two very important topics follows. Creep is the time-dependent deformation under load of a material. The temperature regime for which creep is important is $0.4\,T_m < T < T_m$, T_m being the melting point in Kelvin. In this temperature range, diffusion is a significant factor. Diffusion, being a thermally activated process, shows an exponential dependence. Below $0.5\,T_m$, the diffusivity is so low that any deformation mode exclusively dependent on it can be effectively neglected. Thus, the creep temperature range varies from metal to metal; lead creeps at ambient temperature, while iron creeps above 600°C.

The key to understanding the creep mechanisms is the realization that the activation energies for creep and diffusion are the same for a large number of metals (Fig. 9). The activation energy for diffusion is related to diffusion coefficient D by

$$D = D_0 \exp(-Q_D/kT)$$

For temperatures below $0.5\,T_m$, the activation energy for creep tends to be lower than that for self-diffusion. It is thought at these lower temperatures, diffusion occurs preferentially along dislocations (pipe diffusion), instead of bulk diffusion.

For $T > 0.4\,T_m$, the creep mechanisms can be

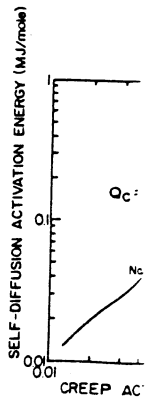

FIG. 9. Activation e self-diffusion for a n Sherby and A. K. Mi **101**, 387.]

divided in four majo applied stress:

(a) *Diffusion cree ble creep).* This ten Nabarro–Herring cr cancies inside grain such a way as to pro the grain along the stress. Coble creep grain boundaries. Th ring and Coble diff pressed as

$$\dot{\varepsilon} = 14\left(\frac{\sigma\Omega}{kT}\right)$$

where D_B and D_v are diffusion coefficients grain size; δ is the gr is the atomic volum have their usual mear

(b) *Dislocation cree* $< \sigma/G < 10^{-2}$, creep tion glide aided by vac developed a theory based on dislocation ling step. The creep ra as

$$\dot{\varepsilon} = \frac{D}{kT}\sigma^n$$

where n has been obse of metals.

(c) *Dislocation glid* cation glide is respons 10^9, the exponent n as

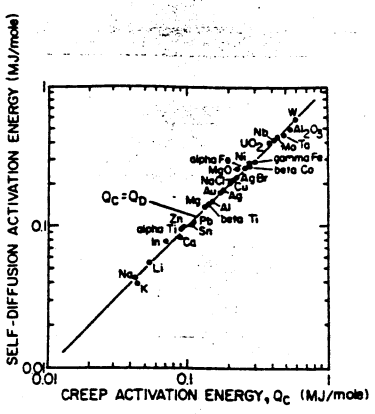

FIG. 9. Activation energies for creep (stage II) and self-diffusion for a number of metals. [After O. D. Sherby and A. K. Miller (1979). *J. Eng. Mater. Tech.* **101**, 387.]

divided in four major groups as a function of the applied stress:

(a) *Diffusion creep (Nabarro–Herring or Coble creep)*. This tends to occur for $\sigma/G \leq 10^{-4}$. Nabarro–Herring creep involves the flux of vacancies inside grains. The vacancies move in such a way as to produce an increase in length of the grain along the direction of applied tensile stress. Coble creep involves diffusion in the grain boundaries. The combined Nabarro–Herring and Coble diffusional creep can be expressed as

$$\dot{\varepsilon} = 14\left(\frac{\sigma\Omega}{kT}\right)\frac{1}{D^2}D_v\left(1+\frac{\pi\delta D_B}{DD_v}\right)$$

where D_B and D_v are the boundary and volume diffusion coefficients, respectively, D is the grain size; δ is the grain-boundary thickness; Ω is the atomic volume; and the other symbols have their usual meaning.

(b) *Dislocation creep*. In the stress range $10^{-4} < \sigma/G < 10^{-2}$, creep tends to occur by dislocation glide aided by vacancy diffusion. Weertman developed a theory for minimum creep rate based on dislocation climb as the rate-controlling step. The creep rate in this case is expressed as

$$\dot{\varepsilon} = \frac{D}{kT}\sigma^n \exp(-Q_D/kT)$$

where n has been observed to be 5 for a number of metals.

(c) *Dislocation glide*. For $\sigma/G > 10^{-2}$, dislocation glide is responsible for creep. For $\dot{\varepsilon}/D > 10^9$, the exponent n assumes a very high value (~10), and transmission electron microscopy work shows that at very high stresses, dislocation climb is replaced by dislocation glide, which does not depend on diffusion.

(d) *Grain boundary sliding*. This deformation mode becomes important in the later stages of creep. It is also an important process in superplasticity where most of deformation occurs by boundary sliding.

A convenient graphical way of representing the various deformation modes in the stress versus temperature space is a so-called deformation mechanism (Weertman–Ashby) map. A typical map for W is shown in Fig. 10. From the deformation-mechanism map, we can determine the dominant mechanism for a certain combination of stress and temperature, find the strain (creep) rate that will result, and devise a strengthening mechanism that is appropriate for the desired portion of the map.

Fatigue is the phenomenon of fracture under cyclic loading. It is a problem that affects any component or part that moves. Automobiles, airplanes, ships, nuclear reactors, turbines, and many other moving components or parts all face the problem of fatigue in one form or another. Traditionally, the material behavior under fatigue conditions has been studied by obtaining S–N curves, where S is the cyclic stress and N is the number of cycles to failure. This is called stress-controlled cycling. When both the maximum and the minimum stresses are below the yield stress, most metals obey Basquin's law,

$$(\Delta\sigma)N^b = C \qquad (12)$$

where $\Delta\sigma$ is the stress cycling range, N is the number of cycles to failure, b is a constant (between 0.07 and 0.1), and C is another constant.

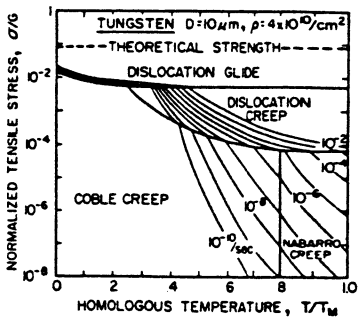

FIG. 10. Weertman–Ashby map for tungsten showing constant strain-rate contours. [After M. F. Ashby (1972). *Acta Met.* **20**, 887.]

The range of validity of this relationship involves a rather large number of cycles, and therefore it is called high-cycle fatigue (HCF). In contrast, we have a low-cycle fatigue (LCF) under strain control where the maximum and the minimum stresses are above yield stress, and we have the relationship called the Coffin–Manson law,

$$(\Delta\varepsilon_p)N^c = C' \qquad (13)$$

where $\Delta\varepsilon_p$ is the plastic strain range, c is a constant (between 0.5 and 0.6), and C' is another constant. Equations (12) and (13) describe the fatigue behavior of smooth, unnotched components.

Fatigue cracks nucleate at discontinuities on the surface or near the surface of a metal. The discontinuities can be structural (such as inclusions, second-phase particles, grain boundaries) or geometrical (such as scratches). These singularities or discontinuities may be present from the beginning or may develop during cyclic deformation. An example of the latter is the formation of intrusions and extrusions at the so-called persistent slip bands (PSBs). Observations of the dislocation structure of the PSBs have shown them to consist of a series of parallel "ledges" (a ladder). These ladders are channels through which the dislocations move and produce intrusions and extrusions at the surface.

Once a fatigue crack is nucleated, its propagation starts in a crystallographic shear mode (a few tenths of a millimeter) and from there on in a direction normal to the maximum principal stress axis in the tensile mode. These two stages have been termed stage I and stage II, respectively. Microscopic observations of fatigue fracture surfaces in stage II for various metals show the appearance of characteristic fatigue striations. Fatigue crack propagation studies are better done using the principles of fracture mechanics, as shown below.

In large structures (in particular, welded structures such as bridges, pressure vessels, oil rigs, etc.), as per fracture mechanics philosophy, there always will be present crack-like defects. Under such circumstances, one asks the question: how many cycles can the structure withstand without one of the preexistent cracks growing to a length at which catastrophic fracture occurs? Fatigue crack propagation studies are thus done on samples containing sharp cracks. One measures the crack growth rate da/dN as a function of cyclic stress intensity factor ΔK (Fig. 11), where $\Delta K = Y\,\Delta\sigma\sqrt{\pi a}$. The curve has a sigmoidal form with a power law connecting the upper and lower limiting region. The power law (region II in Fig. 11) is known as the Paris relationship and has the form

$$da/dN = A(\Delta K)^m \qquad (14)$$

where A and m are constants. In principle, one can integrate Eq. (14) to determine the service life N_f or an appropriate inspection interval ΔN for a structural component. Thus,

$$N_f = \int_{a_0}^{a_f} \frac{da}{A(\Delta K)^m}$$

$$\Delta N = N_2 - N_1 = \int_{a_1}^{a_2} \frac{da}{A(\Delta K)^m}$$

Compilations of da/dN versus ΔK data for various structural materials are available in literature.

A note of caution is in order here. In the above treatment of "long" fatigue crack propagation, the time for crack initiation is assumed to be zero and the plastic zone size is small compared to the crack length. Under such conditions, one determines the crack growth kinetics for a particular material under a given set of conditions and obtains a Paris type relationship describing the crack growth characteristics of the material as given above. As per this formulation, the crack does not propagate below a threshold value, ΔK_{th}. Recently, it has been observed experimentally, however, that "short" fatigue cracks do propagate at $\Delta K < \Delta K_{th}$ (Fig. 12) and that they do not obey a Paris-type growth relationship. By "short" crack here, one means crack length shorter than the physical dimension of the microstructural constituent (l^* in Fig. 12). Clearly, under these conditions, the plastic zone size at the crack tip will not be small

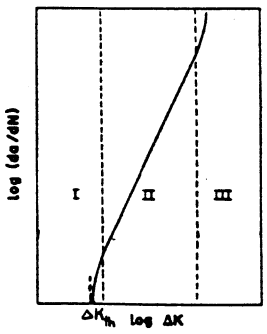

FIG. 11. Crack propagation rate (da/dN) versus alternating stress intensity factor (ΔK) (schematic): stage I, no propagation; II, $(da/dN) = C(\Delta K)^m$; and III, rapid progagation.

FIG. 12. Limiting s
tion of crack length
length l^* propagate

and the material st
not be treated as a
activity is going o
explaining the "an
fatigue cracks.

IV. Mechanica

Mechanical testi
between mechanic
mance. Various me
idealized loading s
late the mechanica
by the metal. The
tained by means of
wit, tensile and co
torsion tests, hardr
tigue tests, creep te
formability tests—s
mechanical perform
structure in real ser

Most of the com
enumerated have
American Society
(ASTM). For speci
ASTM standards,
specifications, etc.,
ASTM. The three
tests are briefly desc

A. Tensile Testing

The design of the
quires the determin
the components. In
temperature is not v
loading is not cyclic
no great concern), th
nents are determined
teria:

(a) excessive elas
(b) plastic deform

h a power law connect-
:r limiting region. The
ig. 11) is known as the
s the form

$$A(\Delta K)^m \qquad (14)$$

tants. In principle, one
determine the service
inspection interval ΔN
nt. Thus,

$$= \int_{a_1}^{a_2} \frac{da}{A(\Delta K)^m}$$

ersus ΔK data for vari-
are available in litera-

in order here. In the
" fatigue crack propa-
initiation is assumed to
one size is small com-
h. Under such condi-
crack growth kinetics
under a given set of
Paris type relationship
wth characteristics of
e. As per this formula-
t propagate below a
cently, it has been ob-
owever, that "short"
te at $\Delta K < \Delta K_{th}$ (Fig.
ot obey a Paris-type
hort" crack here, one
r than the physical di-
tural constituent (l^* in
these conditions, the
ck tip will not be small

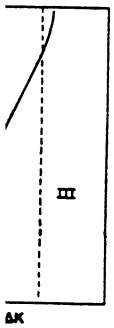

e (da/dN) versus alter-
K) (schematic): stage I,
$C(\Delta K)^m$; and III, rapid

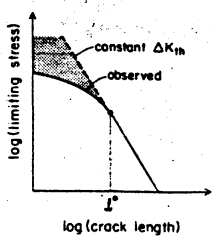

FIG. 12. Limiting stress for fatigue failure as a function of crack length. Cracks shorter than a critical length l^* propagate below ΔK_{th}.

and the material surrounding the crack tip cannot be treated as a continuum. Intense research activity is going on at present with a view to explaining the "anomalous" behavior of short fatigue cracks.

IV. Mechanical Testing

Mechanical testing provides the vital linkage between mechanical properties and performance. Various mechanical tests are nothing but idealized loading sequences designed to simulate the mechanical environment encountered by the metal. The mechanical properties obtained by means of various mechanical tests—to wit, tensile and compressive tests, shear and torsion tests, hardness tests, fracture tests fatigue tests, creep tests, and, last but not least, formability tests—serve as a guideline to predict mechanical performance of a metal as part of a structure in real service.

Most of the common mechanical tests just enumerated have been standardized by the American Society for Testing and Materials (ASTM). For specific information on various ASTM standards, test methods, definitions, specifications, etc., the reader is referred to ASTM. The three most common mechanical tests are briefly described below.

A. Tensile Testing

The design of the structures and systems requires the determination of the dimensions of the components. In applications in which the temperature is not very high and in which the loading is not cyclic (or where load cycling is of no great concern), the dimensions of the components are determined based on four possible criteria:

(a) excessive elastic deformation,
(b) plastic deformation,
(c) excessive plastic deformation, and
(d) unstable crack propagation.

Criterion (a) states that a certain component can undergo a specific maximum elastic strain. The elastic modulus of the material is the important property, since it allows, through Hooke's law, the establishment of the maximum stress. Criterion (b) limits the strains to elastic (recoverable) strains and prohibits plastic strains; the important property of the material is the yield stress. Criterion (c) accepts a certain amount of plastic deformation; important material properties are the ultimate strength, the uniform elongation, and the work hardening. Criterion (d) accepts the possible existence of cracks or defects, and maximum loads are based on fracture mechanics.

These important properties of materials are obtained by means of the tensile test. The tensile test consists of extending a specimen of standardized dimensions at a constant velocity; the load extension of the specimen is recorded and normalized, to represent material properties and not the specific response of the specimen. The load-extension curve is transformed into a stress–strain curve, from which the following material parameters can be extracted; Young's modulus, yield stress (or yield point), ultimate tensile stress, breaking stress, uniform elongation, and total elongation.

Figure 13 shows two typical stress–strain curves. The various parameters are indicated by letters on the curves. The curve shown in Fig. 13(a) shows a gradual transition from elastic to plastic deformation, while the curve shown in Fig. 13(b) shows a yield point followed by a plateau. The elastic modulus of a metal (Young's modulus) is determined by the slope at the linear portion of the stress–strain curve. In Fig. 13, it corresponds to E. On loading, first there is the elastic limit. Since it is difficult to determine the maximum stress for which there is no residual

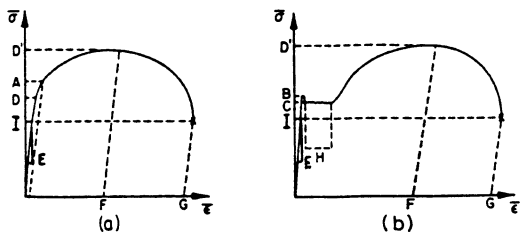

FIG. 13. Engineering (or nominal) stress versus strain curves (a) without and (b) with yield point.

plastic deformation (the linear portion of the stress-strain curve), the 0.2% offset yield stress is defined for materials having a gradual transition from elastic to plastic response. This point is marked as A in Fig. 13(a). It corresponds to a plastic (irrecoverable) strain at 0.002.

In case there is a yield drop, an upper (B) and a lower (C) yield point are defined. A proportionality limit is also sometimes defined (D); it corresponds to the stress at which the curve deviates from linearity. The maximum engineering stress, that is, force divided by the original cross-sectional area, is called ultimate tensile stress (UTS); it corresponds to point D′ in Fig. 13. Beyond the UTS, the engineering stress drops until the rupture stress (I) is reached. The uniform elongation (F) corresponds to the plastic strain that takes place uniformly in the specimens. Beyond that point, necking occurs. Necking starts at the UTS. Point G gives the total elongation.

B. Hardness Testing

The hardness test, for metallurgists, determines the resistance of a metal to penetration by a pyramidal, conical, or spherical indentor. This penetration involves elastic as well as plastic deformation, and the state of stress/strain surrounding the deformation region is a complex one. The hardness tests provide a number that, in a semiempirical way, describes the strength of the metal. In this sense the hardness is not a fundamental deformation parameter. The hardness test is the most common test applied to metals, mainly because it is very simple, inexpensive, and straightforward. It can provide a preliminary assessment of the effect of previous heat treatments, mechanical treatments, and of the composition of the material. The three most common hardness tests applied to metals are the Rockwell, the Brinell, and the Vickers (or diamond pyramid) tests. In the Brinell and Vickers tests, the diameter of the impression is measured. In the Rockwell test, the testing machine automatically registers the depth of the impression. By means of an appropriate equation, different for each hardness test, this number is converted into a hardness number. For the Brinell test, one has

$$HB = \frac{2P}{\pi D(D - \sqrt{D^2 - d^2})}$$

where P is the load, D is the sphere diameter, and d is the impression diameter. The Brinell test uses spherical indentors. For the Vickers test, one has

$$HV = \frac{1.8554P}{d^2}$$

where P is the load and d is the average length of the diagonals of the square impression. The Vickers test uses a pyramidal indentor with a square base.

In the Rockwell test, the hardness is read directly from a dial in the machine. The load is applied to the indentor (several indentors may be used: $\frac{1}{4}$ in., $\frac{1}{8}$ in., $\frac{1}{16}$ in. spheres, or a diamond cone with 20° cone angle) by means of a lever arm. A preload is applied prior to the main load. The depth of indentation is read on a dial gage. Hence, no equation is needed. The Rockwell test provides an arbitrary number with no units.

C. Fracture Testing

The most important fracture tests can be grouped in two categories: impact tests, and fracture toughness tests. The purpose of fracture testing is to establish the resistance of a metal to fracture. In the impact tests, only the energy absorbed or the extent of cracking after a specified blow are determined. The fracture toughness tests are more quantitative and fundamental. These tests try to obtain fundamental parameters: the plane strain fracture toughness, the energy release rate, the crack opening displacement, the crack-tip opening displacement, and the J integral.

The most common impact test (Charpy) and fracture toughness test are briefly described below.

The Charpy V-notch impact test is ASTM A370. The notch is located in the center of test sample. The test sample, supported horizontally at two points, receives an impact from a pendulum of a specific weight on the side opposite that of the notch [Fig. 14(a)]. The specimen fails in flexure under impact ($\dot{\varepsilon} \approx 10^3$ sec^{-1}).

In the region around the notch in the test piece, there exists a triaxial stress state due to plastic yielding constraint there. This triaxial stress state and the high strain rates used propitiate the tendency for a brittle failure. Generally, one presents the results of a Charpy test as the energy absorbed in fracturing the test piece. An indication of the tenacity of the material can be obtained by an examination of the fracture surface. Ductile materials show a fibrous aspect, whereas brittle materials show a flat fracture.

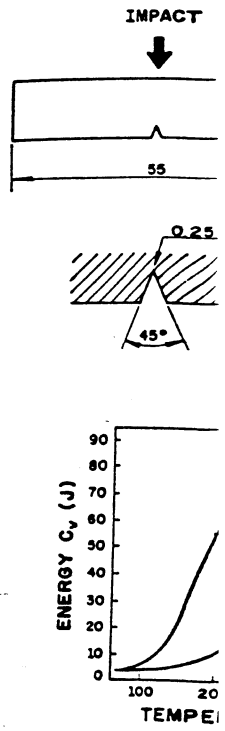

FIG. 14. (a) Charpy imp
meters. (b) Energy absor
steel in annealed and qu
tions.

A Charpy test at onl
sufficient, however, t
sorbed in fracture dr
temperature. Figure 1
of energy absorbed as
for a steel in the annea
and tempered state. T
there occurs a change
ture to a low-energy o
brittle transition temp
ever, as in practice the
change in energy but in
sition zone, it become
DBTT with precision.

Thus, generally a se
temperatures is conduct
termine a transition ten
brittle transition temp
trary, is an important
selection from the poin
the tendency of occurr
As this transition tempe

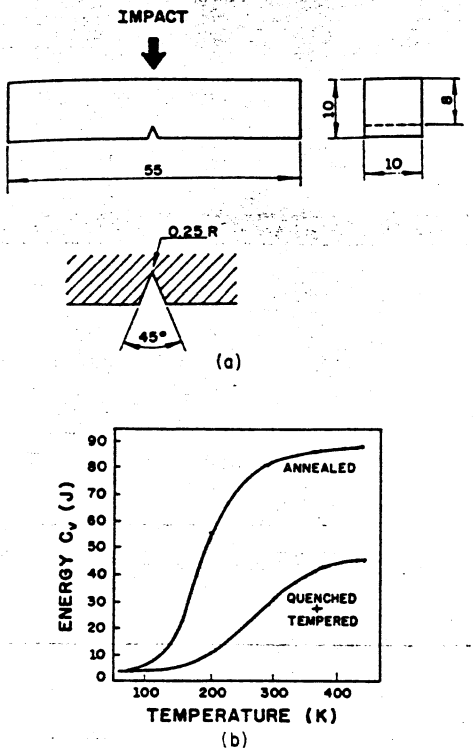

FIG. 14. (a) Charpy impact test; dimensions in millimeters. (b) Energy absorbed versus temperature for a steel in annealed and quenched and tempered conditions.

A Charpy test at only one temperature is not sufficient, however, because the energy absorbed in fracture drops with decreasing test temperature. Figure 14(b) shows this variation of energy absorbed as a function of temperature for a steel in the annealed and in the quenched and tempered state. The temperature at which there occurs a change from a high-energy fracture to a low-energy one is called the ductile–brittle transition temperature (DBTT). However, as in practice there does not occur a sharp change in energy but instead there occurs a transition zone, it becomes difficult to obtain this DBTT with precision.

Thus, generally a series of tests at different temperatures is conducted that permits us to determine a transition temperature. This ductile–brittle transition temperature, however arbitrary, is an important parameter in material selection from the point of view of tenacity or the tendency of occurrence of brittle fracture. As this transition temperature is, generally, not very well defined, there exist a number of empirical ways of determining it, based on a certain absorbed energy (e.g. 15 J), change in the fracture aspect (e.g., the temperature corresponding to 50% fibrous fracture), or lateral contraction (e.g., 1%) that occurs at the notch root. The transition temperature depends on the chemical composition, heat treatment, processing, and microstructure of the material. FCC metals usually do not exhibit a DBTT.

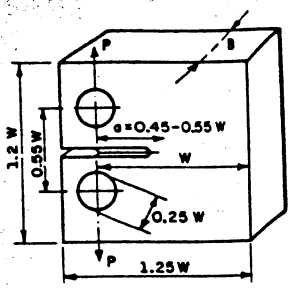

FIG. 15. Compact tension specimen for the determination of the plane-strain fracture toughness.

The plane strain fracture toughness K_{Ic} may be determined according to the standards ASTM E399/79 or BS 5447/77. The essential steps in the fracture toughness tests involve measurements of crack extension and load at the sudden failure of sample. As it is difficult to measure crack extension directly, one measures the relative displacement of two points on the opposite sides of the crack plane. This displacement can be calibrated and related to real crack front extension.

A typical compact-tension sample that is used in the fracture toughness tests according to the ASTM standard is shown in Fig. 15. As the load P is increased, an existing precrack, of length a, is subjected to higher and higher stresses. At a critical value of P the crack will start to grow in an unstable manner. This critical load P is used in the computation of the plane strain fracture toughness. In order for plane-strain conditions to prevail, it is necessary to have a lower limit on specimen thickness. Once the plane-strain fracture toughness of a metal is known, it can be used to compute the maximum stress that this metal will withstand if we know the size of the maximum flaws that it contains. Typical values of plane strain fracture toughness are given in Table I. By applying Eq. (6) one can determine the critical crack size for a certain loading situation or vice versa.

BIBLIOGRAPHY

Avitzur, B. (1984). "Metal Forming: Processes and Analysis." Prentice-Hall, Englewood Cliffs, N.J.

Broutman, L. J., and Krock, R. H., eds. (1971–1975). "Composite Materials," Vols. 1–8. Academic, New York.

Cahn, R. W., and Haasen, P., eds., (1983). "Physical Metallurgy," 3d ed. North-Holland, Amsterdam.

Ewalds, H. L., and Wanhill, R. J. H. (1984). "Fracture Mechanics." Edward Arnold, London.

Gittus, J. (1975). "Creep, Viscoelasticity and Creep Fracture in Solids." Halsted Press (Wiley), New York.

Hertzberg, R. W. (1983). "Deformation and Fracture Mechanics of Engineering Materials," 2nd ed. Wiley, New York.

Hirth, J. P., and Lothe, J. (1981). "Theory of Dislocations," 2nd ed. Wiley, New York.

Korchynsky, M., ed. (1984). "HSLA Steels: Technology & Applications." ASM, Metals Park, Ohio.

Meyers, M. A., ed. (1985). "Metals Handbook (Desk Edition)." Mechanical Testing, Chapter 34, 34.1–42. ASM, Metals Park, Ohio.

Meyers, M. A., and Chawla, K. K. (1984). "Mechanical Metallurgy." Prentice-Hall, Englewood Cliffs, N.J.

METALS, NOBLE—*SEE* NOBLE METALS

METEOR

Robert C. Ree

GLOSSARY

Complex history: C exposed to appr rays both befor lision in space t

Cosmogenic: Prod tions.

Electron volt: Unit eV, that is nece through a potent equal to 1.602 × cosmic rays typi from about a me eV) or less to (GeV) (10^9 eV) p

Exposure age: Leng has been irradiat of cosmic ray p servable record.

Meteoroid: Object i vives passage t sphere and hits th orite.

Noble gases: Eleme krypton, and xen mal temperature a form compounds, in meteorites. Th rare gases or iner

Radionuclide: Atomi and decays to a emission of radia emits an electron cleus. Each radior